THE ASTROPHYSICAL JOURNAL, 524:L119–L123, 1999 October 20
© 1999. The American Astronomical Society. All rights reserved. Printed in U.S.A.

FORMING THE DUSTY RING IN HR 4796A

SCOTT J. KENYON AND KENNETH WOOD
Smithsonian Astrophysical Observatory, 60 Garden Street, Cambridge, MA 02138; skenyon@cfa.harvard.edu, kwood@cfa.harvard.edu
AND
BARBARA A. WHITNEY AND MICHAEL J. WOLFF
Space Science Institute, Suite 23, 1540 30th Street, Boulder, CO 80303-1012; whitney@colorado.edu, wolff@colorado.edu
Received 1999 July 7; accepted 1999 August 12; published 1999 September 17

ABSTRACT

We describe planetesimal accretion calculations for the dusty ring observed in the nearby A0 star HR 4796A. Models with initial masses of 10–20 times the minimum-mass solar nebula produce a ring with a width of 7–15 AU and a height of 0.3–0.6 AU at 70 AU in ~10 Myr. The ring has a radial optical depth of ~1. These results agree with limits derived from infrared images and from the excess infrared luminosity.

Subject headings: circumstellar matter — planetary systems — solar system: formation — stars: formation — stars: individual (HR 4796A)

1. INTRODUCTION

HR 4796A is a nearby A star with a large infrared (IR) excess. Jura (1991) measured the far-IR excess of this wide binary using *IRAS* data. Jura et al. (1995, 1998) associated the excess with the A0 primary and derived the ratio of the far-IR to the stellar luminosity, $L_{\rm FIR}/L_\star \approx 5 \times 10^{-3}$. In 1998, two groups reported extended thermal emission at $\lambda = 20$ μm from a dusty disk with an inner hole at ~40–70 AU, assuming the *Hipparcos* distance of 67 ± 3.5 pc (Jayawardhana et al. 1998; Koerner et al. 1998). Observations with the Near-Infrared Camera and Multiobject Spectrometer (NICMOS) aboard the *Hubble Space Telescope* (*HST*) have revealed a thin annulus of scattered light, with a width of $\lesssim$17 AU at a distance of ~70 AU from the central star (Schneider et al. 1999). With an age of ~10 Myr (Stauffer, Hartmann, & Barrado y Navascues 1995; Barrado y Navascues et al. 1997), the A0 star is older than most pre–main-sequence stars and younger than stars like β Pictoris and α Lyrae with their "debris disks."

The dusty ring in HR 4796A is a challenge to current theories of planet formation. In most planetesimal accretion calculations, planet-sized objects do not form on short timescales at large distances from the central star. Kenyon & Luu (1999, hereafter KL99) estimate formation times of 10–40 Myr for Pluto at 35 AU from the Sun. Achieving shorter timescales at 70 AU in HR 4796A requires large initial masses, which might conflict with masses derived from IR observations. In the inner solar system, planet formation cannot be confined to a narrow ring because high-velocity objects in adjacent annuli interact and "mix" planetary growth over a large area (Weidenschilling et al. 1997). This problem may be reduced at larger distances from the central star, where planetary growth is "calmer."

Our goal in this Letter is to develop planetesimal accretion models that can lead to the dusty ring observed in HR 4796A. We begin in § 2 with Monte Carlo calculations to constrain the geometry and optical depth of dust in the ring. In § 3, we derive plausible initial conditions that produce the observed dust distribution on 10 Myr timescales. These models also satisfy constraints on the dust mass from *IRAS* observations and lead to a self-consistent picture for ring formation. We conclude in § 4 with a brief summary and discussion of the implications of this study for planet formation in other star systems.

2. MODEL IMAGES

Current data constrain the geometry and optical depth of the ring. Near-IR images measure the amount of scattered light from the ratio of the 1.1–1.6 μm radiation to the stellar luminosity, $L_{\rm NIR}/L_\star \approx 2 \times 10^{-3}$ (Schneider et al. 1999). The far-IR luminosity limits the amount of stellar radiation absorbed and reradiated. To construct a physical model, we assume an annulus of width Δa and height z at a distance $a = 70$ AU from the central star. The luminosity ratios depend on the solid angle $\Omega/4\pi = 2\pi a z/4\pi a^2 = z/2a$, the radial optical depth τ, and the albedo ω: $L_{\rm NIR}/L_\star = \tau\omega(z/2a)$ and $L_{\rm FIR}/L_\star = \tau(1-\omega)(z/2a)$. These equations assume gray opacity and scattering in the geometric optics limit. If the annulus contains planetesimals and dust in dynamical equilibrium, $z/\Delta a \lesssim 1$ (Hornung, Pellat, & Barge 1985). Anticipating the results of our coagulation calculations, where $z/a \sim 10^{-2}$, we then have $\omega \approx 0.3$—close to observed values in β Pic (Backman & Paresce 1993)—and $\tau \sim 1$.

We construct scattered-light images using a three-dimensional Monte Carlo code (Wood & Reynolds 1999) with forced first scattering (Witt 1977) and a "peeling-off" procedure (Yusef-Zadeh, Morris, & White 1984). We adopt a dust number density, $n = n_0 e^{-z^2/2H^2} e^{-(a-70)^2/2A^2}$, where the scale height H and scale length A are in units of AU. We assume $\omega = 0.3$ and isotropic scattering (see Fig. 12 of Augereau et al. 1999), and we adjust τ until the models yield $L_{\rm NIR}/L_\star = 1.5 \times 10^{-3}$ for an input H and A. Model images with $\omega\tau$ = constant are identical in the optically thin limit.

Figure 1 compares several models with the NICMOS 1.1 μm image (from FITS data kindly sent by G. Schneider). We convolved Monte Carlo images with a Gaussian point-spread function with FWHM = 0″12 to approximate the 0″12 resolution of NICMOS (Schneider et al. 1999). Model images with $H > 5$ AU (FWHM = 14 AU) or $A > 10$ AU (FWHM = 27 AU) are more extended than the data (Augereau et al. 1999). Our preferred model with $H = 0.5$ AU, $A = 5$ AU, and $\omega\tau = 0.25$ reproduces the size and shape of the NICMOS image as well as the limb brightening observed toward the ring edges. These results match the NICMOS flux ratios best for our adopted geometry; larger H implies smaller $\omega\tau$. The 3 σ limit, $\omega\tau = 0.12$–0.35, agrees with previous estimates (cf. Koerner et al. 1998; Schneider et al. 1999; Augereau et al. 1999). We

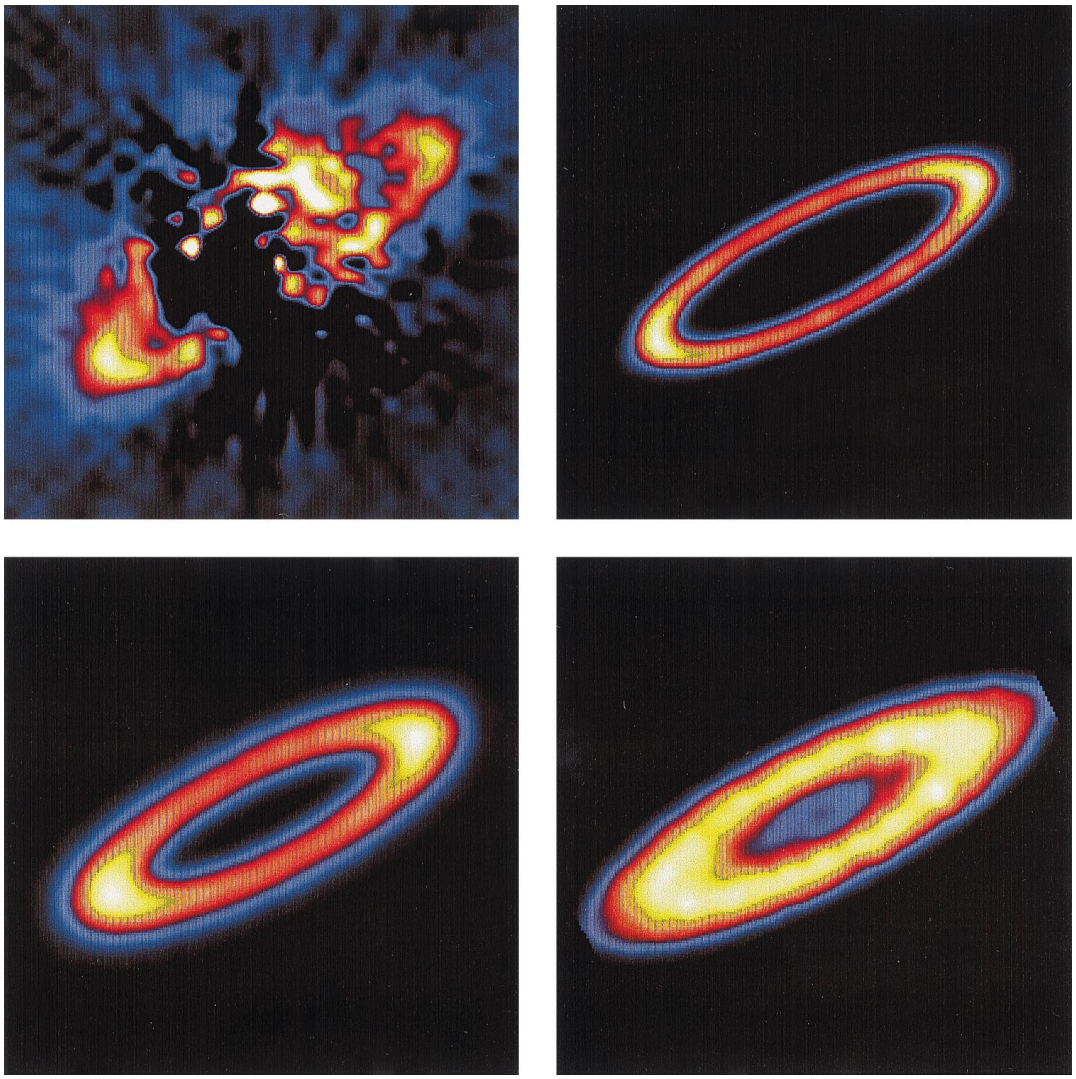

FIG. 1.—Comparison of model scattered-light images with *HST* data of HR 4796A. *Upper left panel*: NICMOS coronagraphic image at 1.1 μm. *Upper right panel*: Model scattered-light image with $z = 0.5$ AU, $R = 5$ AU, and $\omega\tau_{\rm NIR} = 0.25$. *Lower left panel*: The same as in the upper right panel, but for $z = 5$ AU, $R = 10$ AU, and $\omega\tau_{\rm NIR} = 0.02$. *Lower right panel*: The same as in the lower left panel, but for $z = 1$ AU, $R = 20$ AU, and $\omega\tau_{\rm NIR} = 0.1$.

disagree, however, with the $\tau \sim 10^{-3}$ of Schneider et al.; their result is valid only for scattering in a spherical shell.

3. COAGULATION MODEL

To calculate dust evolution in HR 4976A, we use a coagulation code based on the particle in a box method (KL99). This formalism treats planetesimals as a statistical ensemble of bodies with a distribution of horizontal and vertical velocities about Keplerian orbits (Safronov 1969). We begin with a size distribution of N_i bodies having a total mass M_i in each of the i mass batches. Collisions among these bodies produce (1) growth through mergers, along with cratering debris for low-impact velocities, or (2) catastrophic disruption into numerous small fragments for high-impact velocities. Inelastic collisions, long-range gravitational interactions (dynamical friction and viscous stirring), and gas drag change the velocities of the mass batches with time. The code has been tested against analytic solutions of the coagulation equation and published calculations of planetesimal growth. Although inappropriate for the last stages of planet formation, our approach well approximates the early stages (Kokubo & Ida 1996).

We model planetesimal growth in an annulus with a width of $\Delta a = 12$ AU centered at $a = 70$ AU. The central star has a mass of 2.5 $M_\odot$. The input size distribution has equal mass in each of the 38 mass batches with initial radii $r_i = 1$–80 m. For a minimum-mass solar nebula with mass $M_{\rm MMSN}$, the total mass in the annulus is $M_0 \approx 15 M_{\rm E}$ (where $M_{\rm E}$ is the mass of the Earth); the initial number of bodies with $r_i = 1$ m is $N_0 \approx 3 \times 10^{20}$. All batches start with the same initial velocity. The mass density $\rho_0 = 1.5$ g cm^{-3}, intrinsic strength $S_0 = 2 \times 10^6$ ergs g^{-1}, and other bulk properties of the grains are adopted from earlier work (see KL99).

Planetesimal growth at 70 AU follows the evolution described previously (KL99). The 80 m bodies first grow slowly into 1 km objects. During this slow growth phase, frequent collisions damp the velocity dispersion of all the bodies. "Runaway growth" begins when the gravitational range of large objects exceeds their geometric cross section. These bodies grow from 1 up to ~100 km in several megayears. During runaway growth, collisional debris, dynamical friction, and viscous stirring increase the velocity dispersion of small bodies from ~1 up to ~40 m s^{-1}. This evolution reduces the gravi-

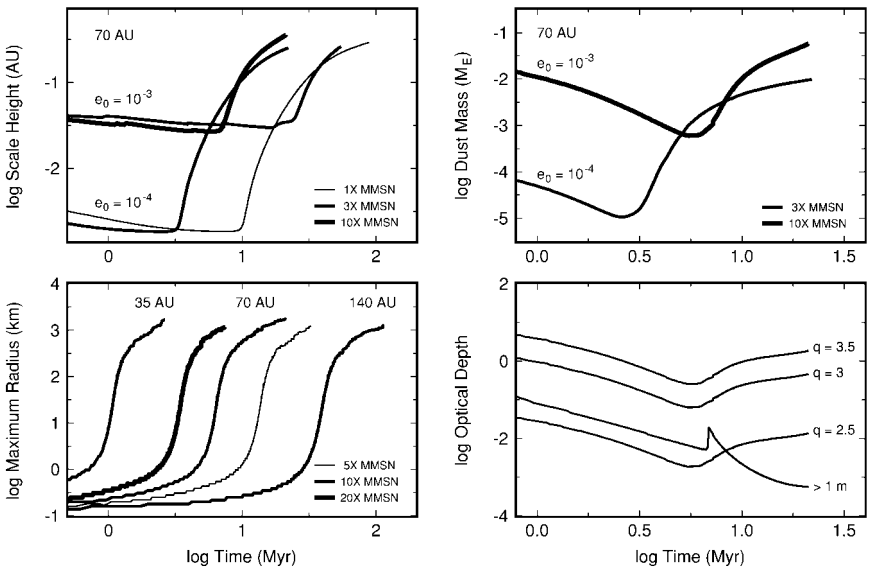

FIG. 2.—Results for HR 4796A coagulation models. *Lower left panel*: maximum radius for models with $e_0 = 10^{-3}$ at $a = 35$, 70, and 140 AU; initial masses are listed in the figure. *Upper left panel*: scale height of small bodies for 70 AU models with e_0 and M_0 as listed. *Upper right panel*: dust mass for 70 AU models with e_0 and M_0 as listed. *Lower right panel*: optical depth for a 70 AU model with $e_0 = 10^{-3}$ and $M_0 = 10M_{\rm MMSN}$.

tational range of the 100 km objects and ends runaway growth. The largest objects then grow slowly to sizes $\gtrsim$1000 km.

The lower left panel of Figure 2 shows the growth of the largest object in several models. For $M_0 = 10M_{\rm MMSN}$ and $e_0 = 10^{-3}$, Pluto-sized objects form in $t_{\rm P} = 2.1$ Myr at $a =$ 35 AU, 13 Myr at 70 AU, and 93 Myr at 140 AU. Models with smaller M_0 take longer to make "Pluto." Plutos form more quickly for $e_0 < 10^{-3}$ because the gravitational focusing factors are larger.

The upper left panel of Figure 2 shows the evolution of the scale height H for small objects. Initially, $H = 2\pi a \sin i \leq 0.003a$ for $e_0 \leq 10^{-3}$. Collisional damping cools the bodies during the slow growth phase; H remains small. H increases dramatically during runaway growth, when dynamical processes heat up the smallest bodies. Once runaway growth ends, H slowly increases to 0.3–0.6 AU independent of M_0, e_0, and other input parameters.

When H begins to increase, high-velocity collisions produce numerous "dust grains" with sizes $\lesssim$1 m. We do not follow explicitly the evolution of these bodies. Instead, we assume that collisional debris is (1) swept up by 1 m or larger objects, (2) ejected by radiation pressure, or (3) dragged inward by the Poynting-Robertson effect. Grains with sizes exceeding 4–5 μm are stable against radiation pressure (Jura et al. 1998; Augereau et al. 1999). Poynting-Robertson drag reduces the mass in small grains on a timescale of $t_{\rm PR} \approx 1.0$ Myr (r_i/4 μm). With the short collision times, $\leq 10^5$ yr, in our model annulus, 1 Myr seems a reasonable estimate of the timescale for collisions to produce 4 μm grains that are removed by radiative processes. For this Letter, we calculate the accretion explicitly and adopt a 1 Myr timescale for dust removal.

The upper right panel of Figure 2 shows the dust mass as a function of time. The results are not sensitive to the adopted mass distribution for grains with $r_i \gtrsim 4$ μm or to a factor of 2–3 variation in the removal timescale. The dust mass is initially large because of the starting conditions. The dust mass decreases with time because (1) collisional damping of the smaller bodies leads to less collisional debris and (2) radiative processes and accretion by large bodies remove dust. Once runaway growth begins, collisions between small bodies produce more dust. The dust mass then reaches a rough equilibrium between dust produced by collisions and dust removed by radiation forces and by the larger bodies.

These results indicate that large dust masses correlate with runaway growth and the formation of one or more Plutos in the outer parts of the disk. To predict the amount of radiation absorbed and scattered by dust and larger bodies, we compute τ from the model size distribution. We assume the geometric optics limit because $r_i \gg \lambda$. For the large bodies, $\tau = \sum_{i=1}^{N} n_i \sigma_i \Delta a$, where n_i is the number density in the mass batch i, σ_i is the extinction cross section, and N is the number of mass batches. We adopt $\sigma_i = 2\pi r_i^2$ and a volume $V_i = 2\pi a \Delta a H_i$ to compute $n_i = N_i/V_i$ and hence τ for material with $r_i \gtrsim 1$ m.

Estimating τ for small particles requires an adopted cumulative size distribution, $N_C \propto r_i^{-q}$. We consider three choices: (1) the collisional limit for coagulation ($q = 2.5$); (2) equal mass per mass interval ($q = 3$); and (3) the approximate distribution for grains in the interstellar medium ($q = 3.5$). Our calculations produce $q \approx 2.7$ for 1–100 m bodies. We expect a slightly steeper mass distribution for smaller bodies because collisions between smaller bodies produce fewer mergers and more debris.

The lower right panel of Figure 2 shows how τ evolves for a single model. The large bodies initially have modest radial optical depth, $\tau_L \approx 0.2$. This optical depth decreases with time, except for a brief period when runaway growth produces 10–100 km objects with a small scale height above the disk midplane. The large bodies are transparent once a Pluto forms. The small grains are also initially opaque. This dust is transparent at late times if most of the mass is in the largest grains, $q \lesssim 2.8$. The dust is opaque for $q \gtrsim 3$.

Table 1 summarizes results for various initial conditions. Models with $M_0 \approx 10$–$20M_{\rm MMSN}$ and $e_0 \approx 10^{-4}$ to 10^{-3} achieve $\tau \sim 1$ in 10 Myr. Less massive disks produce less dust on longer timescales. The results are not sensitive to other input parameters, including the size distribution and the bulk properties of the bodies.

TABLE 1
RESULTS OF PLANETESIMAL ACCRETION CALCULATIONS

a (AU)	M_0 (M_E)	e_0	t_P (Myr)	log τ_S	log τ_L
35	100	10^{-3}	2.1	0.09	−3.43
70	15	10^{-4}	81.1	−1.90	−3.92
	45	10^{-4}	20.4	−0.96	−3.27
	150	10^{-4}	5.8	−0.09	−2.32
	15	10^{-3}	156.4	−2.21	−4.24
	45	10^{-3}	50.0	−1.42	−3.65
	75	10^{-3}	29.9	−0.94	−3.48
	150	10^{-3}	13.0	−0.34	−3.25
	300	10^{-3}	6.6	−0.05	−2.62
140	200	10^{-3}	92.6	−1.20	−2.95

NOTE.—a is the distance of the annulus from the central star; M_0 is the initial mass in the annulus; e_0 is the initial eccentricity of each mass batch; t_P is the timescale for producing Pluto-sized objects; τ_S is the optical depth in dust when the first Pluto forms, assuming equal mass in dust per decade in radius; and τ_L is the optical depth of the large bodies when the first Pluto forms.

Table 1 also shows why dust in HR 4796A lies in a ring. In disks with surface density $\Sigma \propto a^{-3/2}$, the Pluto formation timescale[1] is $t_P \approx 13$ Myr $(M_0/10M_{MMSN})^{-1}(a/70\ \mathrm{AU})^{2.7}$. Once an annulus at a begins to form dust, material at $a + \Delta a$ must wait a time, $\Delta t/t_P \approx 2.7\Delta a/a$, to reach the same state. This result sets a hard outer limit to the ring, $\Delta a/a \approx 0.4\Delta t/t_P \approx 0.1$–$0.2$, if Δt is the time for H to double in size during runaway growth, 2–3 Myr. We expect a hard inner edge because either particle velocities reach the shattering limit of ~100 m s^{-1} (KL99), planets sweep up the dust (e.g., Pollack et al. 1996), or both.

4. DISCUSSION AND SUMMARY

Our results indicate that the dusty ring in HR 4796A is a natural outcome of planetesimal evolution. Planet formation at 70 AU in 10 Myr is possible with an initial disk mass of 10–$20M_{MMSN}$. Dust production associated with planet formation is then confined to a ring with $\Delta a \approx 7$–15 AU. The optical depth in this ring satisfies current constraints on scattered light at 1–2 μm and on thermal emission at 10–100 μm if the size distribution of the dust is $N_C \propto r_i^{-q}$ with $q \gtrsim 3$ for $r_i \lesssim 1$ m. Models with disk masses smaller than $10M_{MMSN}$ fail to produce planets and an observable dusty ring in 10 Myr.

An uncertainty in our model is the timescale for producing 1–80 m bodies from small dust grains in a turbulent, gaseous disk. Cuzzi, Dobrovolskis, & Champney (1993) show that grains grow very rapidly once they decouple from eddies in the disk. The decoupling timescale depends on the unknown disk viscosity at 70 AU.

Our model makes several observational predictions. We expect $L_{NIR}/L_\star$ = constant for $\lambda \leq 5$ μm; current data are consistent with this prediction at the 1.5 σ level. Better measurements of the ring flux at $\lambda \geq 1.6$ μm would test our optical depth assumptions and yield interesting constraints on grain properties. Deep images at $\lambda \geq 10$–20 μm with high spatial resolution should detect material outside the ring. We predict $\tau \approx 0.1$ in large bodies for $a \gtrsim 80$ AU; the surface brightness and temperature of this material should decrease markedly with radius. This material should have negligible mass in small objects because coagulation concentrates mass in the largest objects when H is small. We also expect a flux of dust grains to flow into the central star, although we cannot yet compare quantitative predictions with observations. Future calculations of radiative processes within the ring will address this issue.

Applying this HR 4796A model to other stars with circumstellar disks is challenging because of small-number statistics and unfavorable circumstances. Nearby companion stars probably influence the dynamics of dusty rings in HD 98800 and HD 141569 (Pirzkal, Spillar, & Dyck 1997; Low, Hines, & Schneider 1999; Lagrange, Backman, & Artymowicz 1999). In HR 4796A, the M-type companion lies well outside the ring radius and cannot modify ring dynamics significantly. Older systems like β Pic and α Lyr require the time-dependent treatment of dust to allow the ring to spread with time (e.g., Artymowicz 1997). We plan to incorporate this time-dependent behavior in future calculations to see whether the ring in HR 4796A can evolve into a debris disk (as in, e.g., β Pic and α Lyr) on a timescale of 100–200 Myr.

The main alternative to in situ ring formation at 70 AU is the migration of a planet formed at a smaller radius. Weidenschilling & Marzari (1996) show that gravitational interactions can scatter large objects into the outer disk in less than 1 Myr. Migration reduces the required ring mass by a factor of 10–100. However, the scattered body has a large eccentricity, $e \sim 0.5$. Dynamical friction might circularize the orbit in 10 Myr but would induce large eccentricities in smaller bodies. The width of the dusty ring would probably exceed observational constraints. Future calculations can address these issues.

[1] Pluto is a handy reference: objects with sizes ≳1000 km form roughly in the middle of the rapid increase in H that produces large dust masses.

We thank B. Bromley for helping us run our code on the HP Exemplar "Neptune" at JPL and for a generous allotment of computer time through funding from the NASA Offices of Mission to Planet Earth, Aeronautics, and Space Science.

REFERENCES

Artymowicz, P. 1997, Annu. Rev. Earth Planet. Sci., 25, 175
Augereau, J. C., Lagrange, A. M., Mouillet, D., Papaloizou, J. C. B., & Grorod, P. A. 1999, A&A, 348, 557
Backman, D. E., & Paresce, F. 1993, in Protostars and Planets III, ed. E. H. Levy & J. I. Lunine (Tucson: Univ. Arizona Press), 1253
Barrado y Navascues, D., Stauffer, J. R., Hartmann, L., & Balachandran, S. C. 1997, ApJ, 475, 313
Cuzzi, J. N., Dobrovolskis, A. R., & Champney, J. M. 1993, Icarus, 106, 102
Hornung, P., Pellat, R., & Barge, P. 1985, Icarus, 64, 295
Jayawardhana, R., et al. 1998, ApJ, 503, L79
Jura, M. 1991, ApJ, 383, L79
Jura, M., Ghez, A. M., White, R. J., McCarthy, D. W., Smith, R. C., & Martin, P. G. 1995, ApJ, 445, 451
Jura, M., Malkan, M., White, R., Telesco, C., Pina, R., & Fisher, R. S. 1998, ApJ, 505, 897
Kenyon, S. J., & Luu, J. X. 1999, AJ, in press (astro-ph/9904115) (KL99)
Koerner, D. W., Ressler, M. E., Werner, M. W., & Backman, D. E. 1998, ApJ, 503, L83
Kokubo, E., & Ida, S. 1996, Icarus, 123, 180
Lagrange, A. M., Backman, D., & Artymowicz, P. 1999, in Protostars and Planets IV, ed. V. Mannings, A. P. Boss, & S. S. Russell (Tucson: Univ. Arizona Press), in press
Low, F. J., Hines, D. C., & Schneider, G. 1999, ApJ, 520, L45
Pirzkal, N., Spillar, E. J., & Dyck, H. M. 1997, ApJ, 481, 392
Pollack, J. B., Hubickyj, O., Bodenheimer, P., Lissauer, J. J., Podolak, M., & Greenzweig, Y. 1996, Icarus, 124, 62

Safronov, V. S. 1969, Evolution of the Protoplanetary Cloud and Formation of the Earth and Planets (Moscow: Nauka) (English tech. transl., NASA TT F-677 [1972])
Schneider, G., et al. 1999, ApJ, 513, L127
Stauffer, J. R., Hartmann, L. W., & Barrado y Navascues, D. 1995, ApJ, 454, 910
Weidenschilling, S. J., & Marzari, F. 1996, Nature, 384, 619
Weidenschilling, S. J., Spaute, D., Davis, D. R., Marzari, F., & Ohtsuki, K. 1997, Icarus, 128, 429
Witt, A. N. 1977, ApJS, 35, 1
Wood, K., & Reynolds, R. J. 1999, ApJ, in press (astro-ph/9905289)
Yusef-Zadeh, F., Morris, M., & White, R. L. 1984, ApJ, 278, 186